

UCLA

UCLA Previously Published Works

Title

Torsional control of stereoselectivities in electrophilic additions and cycloadditions to alkenes

Permalink

<https://escholarship.org/uc/item/0th6x72x>

Journal

Chemical Science, 5(2)

ISSN

2041-6520

Authors

Wang, Hao
Houk, KN

Publication Date

2014-02-01

DOI

10.1039/c3sc52538d

Peer reviewed



Published in final edited form as:

Chem Sci. 2014 February ; 5(2): . doi:10.1039/C3SC52538D.

Torsional Control of Stereoselectivities in Electrophilic Additions and Cycloadditions to Alkenes

Hao Wang and K. N. Houk*

Department of Chemistry and Biochemistry, University of California, Los Angeles, CA 90095-1569, USA

Abstract

Torsional effects control the π -facial stereoselectivities of a variety of synthetically important organic reactions. This review surveys theoretical calculations that have led to the understanding of the influence of the torsional effects on several types of stereoselective organic reactions, especially electrophilic additions and cycloadditions to alkenes.

Introduction and Background

Stereoselectivity is an essential requirement for the efficient synthesis of stereochemically complex molecules. The control of π -facial selectivity in organic reactions has been a subject of both experimental¹ and theoretical studies.² The origin of π -facial selectivity has been attributed to several factors such as electrostatics,³ hyperconjugation,⁴ steric⁵ and torsional effects.⁶ In the absence of charged or highly polar groups, torsional effects can have a remarkably large influence on stereoselectivity. Torsional strain occurs when vicinal bonds are placed in an eclipsed conformation instead of the more stable staggered conformation. The barrier to rotate between staggered conformations of ethane is 3 kcal/mol. It was initially believed that the barrier to rotation was due to steric interactions between vicinal hydrogens. The distance between the pair of eclipsed Hs is 2.3 Å, less than the sum of the van der Waals radii (2.4 Å). Later, the staggered conformation was identified to be more stable than the eclipsed conformation due to hyperconjugation.⁷ Closed-shell repulsion between filled CH bond orbitals (steric effect) destabilizes the eclipsed conformation, while hyperconjugation between a CH σ bond and an antiperiplanar vicinal CH σ^* orbital stabilizes the staggered conformation. Both effects have been cited to explain this 3 kcal/mol difference, and the relative importance of steric effects and hyperconjugation has been hotly contested.⁸ We take the position that both are important, while the relative contributions depend on the substituents (e.g. steric effects dominate in n-butane, but hyperconjugation in 1,2-difluoroethane).

“Torsional steering” has been used to describe how these torsional effects influence the direction of attack of a reagent on one face of a π -system.⁹ Torsional effects steer the reactant to approach the π -system in a manner that minimizes eclipsing interactions at the reaction center. The importance of a staggered arrangement with respect to forming bonds was first identified by Felkin in 1968 for nucleophilic additions to cyclohexanones.¹⁰ In the absence of steric hindrance, lithium aluminum hydride or other nucleophiles prefer to attack cyclohexanone from the axial direction in order to minimize torsional strain in the transition state, leading to the equatorial alcohol as the product (Figure 1). Felkin also showed how this staggered transition state model could explain the stereoselectivity trends in hydride

reduction of a series of substituted ketones.¹¹ Felkin's discovery was later supported theoretically by Anh and Eisenstein,¹² and their findings subsequently evolved to what is known as the Felkin-Anh model, which describes the transition state for nucleophilic attack on α -chiral carbonyl compounds.¹³ In the Felkin-Anh model, the carbonyl compounds exhibit a staggered conformation, with the largest substituent, L, placed perpendicular to the plane of the carbonyl group, and anti to the attacking nucleophiles. The nucleophile attacks the carbonyl group at the Bürgi–Dunitz angle¹⁴ preferentially from the least hindered trajectory, which is from the side of the smallest substituent to avoid the steric repulsion between the nucleophiles and the chiral center (Figure 2). Before the Felkin-Anh model, two other models were proposed by Cram¹⁵ and Karabatsos,¹⁶ respectively, to rationalize such stereoselective 1,2-inductions, and these are shown in Figure 2. They differ from the Felkin-Anh model in the conformation of the chiral center and the positions of large (L), medium (M), small (S) substituents. In Cram's model, there is an eclipsed conformation between the carbonyl substituent (R) and the largest α -carbonyl substituent (L), while the Karabatsos model has M approximately eclipsed with the carbonyl group, which is found in carbonyl compounds in solution.

Torsional effects have also been used to interpret and predict the stereochemistry in other cases. Toromanoff has applied torsional angle notations as a tool to analyze the reactions involving 5-, 6- and 7-membered unsaturated rings, and also to predict the stereochemistries for related reactions.¹⁷ Another example where torsional effects determine the stereoselectivity was the Fürst-Plattner rule (also known as the trans-diaxial effect), which describes the stereoselective addition of nucleophiles to cyclohexene epoxide.¹⁸ Cyclohexene epoxides undergo ring opening with nucleophiles to give diaxial products as major products, while the thermodynamically more stable diequatorial products are not observed (Figure 3). This is due to the preference of cyclohexanes to adopt the chair conformation over the twist-boat conformation. There are disfavored torsional strains involved in the twist-boat conformation, causing it to have a higher energy than the chair conformation.

While such effects have often been described in terms of product stability (Figure 3), we have shown that torsional effects in transition states are fully capable of explaining the selectivities, consistent with the fact that differences in transition state energies control kinetic selectivities. We have studied models for addition reactions to alkenes. We studied the transition structures for additions of an electrophile, BH_3 , a nucleophile, H^- , and a radical, H^\cdot , to propene. All three approaches are found to involve conformations where the allylic CH bonds are staggered with respect to the forming bond. The general staggered model was also applied to understand asymmetric reactions.¹⁹

In order to rationalize and predict the stereoselectivities for organic reactions, different research groups have proposed a variety of different models. Dannenberg's review in 1999 summarizes these models and concludes that it is difficult to come up with a general model for organic stereoselectivities.²⁰ The torsional model we review here is the dominant factor in many reactions, and contributes to most stereoselectivities, but sometimes in competition with steric and electrostatic factors. In this minireview, we describe theoretical investigations of many examples where torsional effects in transition states control stereoselectivities. We also provide examples where steric effects override torsional effects.

Stereoselectivities of Cycloadditions to Norbornenes

Additions to norbornene provide classic examples of stereoselectivity control by torsional effects. When attacked by various reagents, norbornene **1** and many derivatives show unusually high reactivity and exo stereoselectivity.^{21–24} Huisgen studied the cycloadditions

of norbornene and attributed the unusual exo reactivity displayed by norbornene to “factor X”, at the time an unknown factor.²⁴ The high exo stereoselectivity was rationalized by our group to be caused mainly by torsional effects,²⁵ as shown in the side view in Figure 4. When attacked from the endo face, Newman projection of C1-C2 bond shows a nearly eclipsed arrangement of the partially forming bond. In contrast, exo attack involves a more staggered arrangement in the transition state. Torsional strain differences influence the relative energies of diastereomeric transition states; exo-attack is more favorable than the endo-attack.

Schleyer was the first to note such effects in his studies of norbornyl solvolysis.²⁶ He noted the fact that the C₁H and C₂H bonds become eclipsed upon solvolysis of endo leaving groups, but staggered with exo leaving groups. Our group used rather crude theoretical calculations in the 1980s to determine that torsional effects control the stereoselective cycloaddition of norbornene with fulminic acid.²⁷ Transition states of the concerted cycloaddition of fulminic acid to norbornene were located by MM2 calculations calibrated for transition states from simple quantum mechanical calculations on model systems. Figure 5 shows the direction of bond formation for attack of C or O terminus of fulminic acid on norbornene. Exo attack on norbornene involves a staggered conformation between the forming bonds and the allylic C-C bond with a dihedral angle of 69°, whereas the endo attack of norbornene occurs with a more eclipsing orientation with a dihedral angle of 34° between the forming bonds and the allylic C-H bond. The Schleyer effect is also present in this case. Similarly, our group and Jorgensen found that the high exo stereoselectivities of reactions of syn-sesquinorbornene are also due to torsional effects.²⁸

More recently, we reinvestigated the 1,3-dipolar cycloaddition of norbornene with phenyl azide, a reaction that was studied experimentally by Huisgen.²⁹ He and co-workers found norbornene and its derivatives have a large preference for exo cycloadditions in reactions with phenyl azide and other 1,3-dipoles;²⁴ other groups have reported similar observations.³⁰ It is now possible to do full quantum mechanical calculations even on these larger systems, and our calculations showed that torsional effects are also the stereocontrol elements here.³¹ Figure 6 shows Newman projections along the left C-C bond in the 1,3-dipolar cycloaddition transition states of norbornene and phenyl azide, and the high exo stereoselectivity identified here arises from torsional strain differences in the exo and endo transition states. The exo-attack transition structure occurs with a staggered arrangement along the C-C bond (Figure 6, left). By contrast, the Newman projections for the endo cycloaddition (Figure 6, right) show a severe eclipsed conformation of HCCH. Such torsional strain differences lead the exo-attack TS to be more favorable than the endo-attack TS by 7.4 kcal/mol using M06-2X calculations.

Besides norbornene itself, some other norbornene derivatives such as cyclopropene fused norbornene **2**, cyclobutene fused norbornene **3** and syn-sesquinorbornene **4** (Figure 7) were studied, and the stereochemical outcome for exo cycloadditions was also found to be due to torsional effects. All the exo TSs are calculated to be more stable than the endo TSs, and torsional strain differences between exo and endo-attack TSs are similar to that observed in the norbornene **1** TSs.

We also applied the distortion/interaction model³² to study the reactivities of these norbornene derivatives. Calculations showed a good correlation between the activation barriers (ΔE) and transition state distortion energies (ΔE_d). The substrates **2**, **3**, **4** are all highly strained alkenes, and they are pyramidalized by 45°, 21°, 16°, respectively. It requires less distortion energy to achieve the transition state if the alkene is more pyramidalized, and the activation energy is reduced as a result. Alkene pyramidalization is influenced by torsional effects, and influences distortion as well.

In contrast with the facial selectivity observed for norbornene and its derivatives, isodicyclopentadiene has a high preference for Diels-Alder cycloadditions with various dienophiles from the bottom face (Figure 8).³³ Brown and Houk found that this π -facial stereoselectivity is also a result of torsional effects.³⁴

Transition states of the Diels-Alder reaction of isodicyclopentadiene with ethylene were located, and Figure 9 shows the Newman projections along C2-C3 bond for top and bottom attack. In the optimized structure of isodicyclopentadiene, the dihedral angle of C1C2C3H3 is 19° (Figure 9, middle), top attack leads to a bent down geometry of the norbornene moiety and the dihedral angle of C1C2C3H3 decreases to 14° (Figure 9, left). By contrast, for bottom attack where the norbornene moiety exhibits a bent up geometry, the dihedral angle of C1C2C3H3 increases to 27°, giving a more staggered arrangement (Figure 9, right). Such torsional strain differences make the bottom attack to be 0.5 kcal/mol more favorable than the top attack.

Stereoselectivities of Reactions of Cyclopentene Systems

Norbornene is a cyclopentene forced into a pronounced envelope conformation. Torsional effects are also found to influence the stereoselectivities in the electrophilic additions to cyclopentenes fused in other ways to additional rings.

Cheong and Houk determined that torsional steering is the stereocontrolling element in Danishsky's asymmetric epoxidation step shown in Figure 10.⁹ Danishsky's group showed that the epoxidation of guanacastepene **A** precursor **5**, which consists of a fused cyclopentene, takes place exclusively from the β -face to give β -epoxide **6** as the major product.³⁵ This is surprising since it appears from the drawing of **5**, that the ¹Pr and Me substituent should block the β -face. However, DFT calculations predicted that the β -epoxidation transition state **TS5 β** is lower in energy than the analogous α -epoxidation transition state **TS5 α** by 2.6 kcal/mol. The remarkable difference in activation barriers is a result of different torsional strains involved in the transition states. As shown in the Newman projections of the highlighted blue bond (oval insets in Figure 10), in contrast to the more staggered arrangement in the preferred **TS5 β** , there is severe eclipsing in the unfavorable **TS5 α** with more torsional strain. The corresponding β -epoxidation product was calculated to be more stable than the α -epoxidation product by 3.0 kcal/mol.

More recently, we collaborated with Overman's group to identify the origins of stereoselectivities in an asymmetric dihydroxylation of *cis*-heterobicyclo[3.3.0]octene intermediate, **7**, involved in a total synthesis of chromodorolide **A**.³⁶ The reaction of **7** with OsO₄ gave mixtures of the dihydroxylated products **8a** and **8b**, in which the electrophile approaches the fused cyclopentene from either the concave or convex face, respectively (Figure 11). The major product **8a** is the result of electrophilic addition from the concave face, which appears to be more sterically hindered.

Consistent with the experimental observations, B3LYP calculations predicted that the β -dihydroxylation transition structure **TS7 β** , in which the OsO₄ attacks the sterically more hindered convex face, is more stable than the α -dihydroxylation transition structure **TS7 α** by 2.2 kcal/mol (Figure 12). The different energies of the two transition structures also results from torsional effects. As shown in Figure 12, there is slight torsional difference between **TS7 β** and **TS7 α** (red box insets) at the left C-C bond (shown in red). Torsional differences are more pronounced at the right C-C bond (shown in green), since this bond is more fully formed in the transition state. The α -attack **TS7 α** occurs with a substantial eclipsing conformation, whereas β -attack **TS7 β** involves a more staggered conformation. As

a result, torsional effects overwhelm steric effects, and attack of the electrophile occurs from the sterically more hindered concave face.

Such striking torsional strain differences in the transition states originate from the constrained conformation of this bicyclic cyclopentene substrate. From the Newman projections of the highlighted green bond in the optimized structure of *cis*-bicyclo[3.3.0]octene **7**, there is a 42° dihedral angle difference between the β and α face (Figure 13), leading the β -face attack to be torsionally more favored than the α -face attack. Such torsional arrangements in the reactant are maintained in the transition states (blue and yellow box insets in Figure 13).

We also studied three related *cis*-bicyclo[3.3.0]octene systems, **7a**, **7b**, **7c** that had been explored experimentally in the literature. While **7a** and **7b** give concave face attack selectivity in dihydroxylation, **7c** reacts by convex face attack (Figure 14). The difference arises because conformational flexibility of the substrates influences the stereoselectivities. Whereas **7a** has only one energy minimum, two different low-energy conformations are available for compounds **7b** and **7c**. The previous discuss **7**, and **7a**, have only one major conformer. Here torsional effects are quite different for attack on the two faces, and override other factors and steer attack to the concave face. However, **7b** and **7c** have two major conformers, with the cyclopentene envelope flap either up or down (see Figure 14). They have similar energies and so either concave or convex attack can be staggered. Consequently, the stereoselectivities are no longer controlled by torsional effects, since the electrophile can attack both faces of the cyclopentene envelope with similar torsional strain. Other factors, possibly the electrostatic interactions between the carbonyl carbon and attacking OsO₄ in **7b**, and the steric effects in **7c**, are likely to control the selectivities. As a result, for these conformationally flexible molecules, the stereoselectivity is not determined by torsional effects, but by other factors such as steric and electrostatic interactions.

A related example where the torsional effects control the diastereoselectivities of alkylations of bicyclic malonates intermediates during a total synthesis of sorbicillactone **A** was recently published by Harned.³⁷ He and co-workers have found that the alkylation of cyclohexadienone-derived bicyclic malonates **9** with MeI proceeded preferentially from the concave face to give a 5.5:1 endo/exo ratio of the products (Figure 15).

In line with the experimental observations, M06-2X calculations predict the endo approach to be 0.4 kcal/mol more favorable than the exo approach. In this case, torsional effects determine the different stabilities of the two diastereomeric TSs. In the calculated endo transition state, the dihedral angle of C1C6C7C9 is 75°. By contrast, the exo transition state has a more eclipsed conformation along the C7–C6 bond with the dihedral angle of C1C6C7C9 to be 15°.

A much less constrained 5-membered ring alkene exhibits some selectivity in electrophilic reactions on a pyrrolidinone enolate. Meyers and co-workers found that the enolate of pyrrolidinone **10** reacts with benzyl bromide at -78 °C to give 99% of the α -alkylated product **12** (Figure 17).³⁸ Blake reported a computational study to investigate the origins of the observed high α -stereoselectivity for this alkylation reaction.³⁹ Two different conformations of the enolates, **11a** and **11b**, were located for the pyrrolidinone, and **11b** was 3.0 kcal/mol more stable than **11a** due to the strong 1,2-interactions between two methyl groups in **11a**. Transition states for electrophilic reactions of enolate **11b** with methyl bromide showed that α -attack is favored over β -attack by 1.0 kcal/mol. The lack of steric or chelation factors led the author to conclude that the high stereoselectivity arises from the unsymmetrical lone pair of the enolate.

The Houk group reinvestigated this reaction using HF quantum mechanical calculations.⁴⁰ The two alkylation transition states located by HF calculations are shown in Figure 18; these are similar to those reported by Blake.^{39a} The α -attack was favored over β -attack by 1.7 kcal/mol. Torsional effects were identified as the stereocontrol element. From the Newman projections of the highlighted red bond (Figure 18), it is clear that β -attack TS involves an eclipsed conformation of all the vicinal bonds, in contrast to the nearly perfectly staggered arrangement in the α -attack.

Based on this explanation, and the proposal that the lone pair extension had no role, it was predicted that the corresponding trans-2,3-dimethylcyclopentanone would behave like the pyrrolidinone. The Houk group synthesized the corresponding cyclopentanone, and established that the same α -stereoselectivity occurred upon alkylation of the enolate.⁴⁰

Stereoselectivities of Reactions of 5-, 6-, and 7-Membered Cyclic Styrenes

Torsional steering was also found to control stereoselectivity in the electrophilic epoxidations of π -bonds of cyclic styrenes.

Martinelli and co-workers at Eli Lilly prepared several styrene derivatives and investigated their stereoselectivities in epoxidations.⁴¹ Three substrates, **14**, **15** and **16**, differing by ring sizes, were epoxidized. When **14** was oxidized by m-CPBA, remarkably high α -attack stereoselectivities were observed. By contrast, **15**, containing a seven-membered ring, gave primarily β -stereoselectivity with the same oxidation conditions. There was no selectivity for the epoxidation of **16** (Figure 19).

Computational studies were performed on these systems with empirical force field calculations. Torsional effects were proposed as the stereocontrolling elements here.⁴² MM2 optimized structures of compounds **14**, **15** and **16** shown in Figure 20 indicate that the conformation of the reactants influences the reaction stereoselectivities. Compound **14** has a half-chair conformation for the six-membered ring, and this conformation leads the β face to be torsionally disfavored, as shown in the Newman projection **14NP**. Electrophilic attack from the β face suffers severe eclipsing between the forming bond and the axial CH bond and is unfavorable. Here, torsional steering overrides steric effects, leading the electrophile to attack from the more crowded α face. By contrast, in **15**, the seven-membered ring adopts an envelope conformation in which the torsional strains are opposite to that of **14**. As shown in **15NP**, the β face is more crowded, however, torsional effects still steer the electrophilic attack from this face in order to avoid the disfavored eclipsing conformation in the α -attack TS. Unlike **14** and **15**, the five-membered ring in the optimized structures of compound **16** is nearly planar, which leads to little torsional strain difference between the β and α face, as shown in **16NP**. As a result, no stereoselectivity is observed for epoxidation of this compound.

In order to provide energetic information about the importance of torsional effects on the control of π -facial stereoselectivity, transition states of epoxidations of **14**, **15** and **16** were computed with PM3, a semi-empirical quantum mechanical method, a level computationally feasible at that time.⁴³ Figure 21 shows the PM3 optimized diastereomeric transition structures for the epoxidations of three different substrates; single point energy calculations were performed using RHF/6-21G*. For compound **14**, the α -attack **TS14 α** is calculated to be more stable than the β -attack **TS14 β** by 2.1 kcal/mol. This energy difference between two transition states is due to the torsional destabilization of transition structure **TS14 β** . By contrast, the same model calculations gave a 0.9 kcal/mol preference for β -epoxidation on **15**. Here, the cycloheptene has an envelope conformation, and the α -attack results in a more eclipsing interaction, which is disfavored. For compound **16**, however, the two

diastereomeric transition states were calculated to be similar in energy. As shown in the optimized transition structures of **TS16 α** and **TS16 β** , the cyclopentadiene ring is nearly planar; as a result, similar torsional strains are present in **TS16 β** and **TS16 α** . For these three substrates, torsional strain differences shown in the two diastereomeric transition states are consistent with the torsional strain analysis on reactants.

Conclusions

Torsional effect has been identified as a general stereocontrolling element in a variety of stereoselective additions and cycloadditions. Torsional factors can efficiently steer electrophiles and cycloaddends of all types towards attack on one face of the π -system. Computational studies have provided insights into how torsional effects can influence stereocontrol in the transition state. The scope of the reactions reported in this review suggests wide applicability of the general principle of torsional steering in stereoselectivity of additions and cycloadditions to π -systems. While conventional steric and electrostatic effects also influence stereoselectivity, the importance of staggering in transition state for additions and cycloadditions is a universal feature of these reactions.

Acknowledgments

We are grateful to the National Institute of General Medical Sciences, National Institutes of Health, and the National Science Foundation for financial support of our research.

References

1. Kolodiaznyi OI. *Tetrahedron*. 2003; 59:5953.
2. Houk KN, Paddon-Row MN, Rondan NG, Wu Y-D, Brown FK, Spellmeyer DC, Metz JT, Li Y, Loncharich RJ. *Science*. 1986; 231:1108. [PubMed: 3945819]
3. a Wong SS, Paddon-Row MN. *Aust. J. Chem.* 1991; 44:765.b Kahn SD, Pau CF, Chamberlin AR, Hehre WJ. *J. Am. Chem. Soc.* 1987; 109:650.
4. a Hahn JM, Le Noble WJ. *J. Am. Chem. Soc.* 1992; 114:1916.b Le Noble WJ, Lin MH, Silver JE. *J. Org. Chem.* 1988; 53:5155.c Halterman RL, McEvoy MA. *J. Am. Chem. Soc.* 1992; 114:980.d Cieplak AS, Tait BD, Johnson CR. *J. Am. Chem. Soc.* 1989; 111:8447.
5. a Brown HC, Hammar WJ, Kawakami JH, Rothberg I, Van der Jugt DL. *J. Am. Chem. Soc.* 1967; 89:6381.b Brown HC, Kawakami JH, Liu KT. *J. Am. Chem. Soc.* 1973; 95:2209.c Wang H, Michalak K, Michalak M, Jimenez-Oses G, Wicha J, Houk KN. *J. Org. Chem.* 2010; 75:762. [PubMed: 20039618]
6. a Wu Y-D, Tucker JA, Houk KN. *J. Am. Chem. Soc.* 1991; 113:5018.b Wu Y-D, Houk KN. *J. Am. Chem. Soc.* 1987; 109:908.c Vedejs E, Dent WH. *J. Am. Chem. Soc.* 1989; 111:6861.
7. Weinhold F. *Nature*. 2001; 411:539. [PubMed: 11385553]
8. a Bickelhaupt FM, Baerends EJ. *Angew. Chem., Int. Ed.* 2003; 42:4183.b Weinhold F. *Angew. Chem., Int. Ed.* 2003; 42:4188.
9. Cheong PH, Yun H, Danishefsky SJ, Houk KN. *Org. Lett.* 2006; 8:1513. [PubMed: 16597098]
10. Cherest M, Felkin H. *Tetrahedron Lett.* 1968; 9:2205.
11. Cherest M, Felkin H. *Tetrahedron Lett.* 1971; 12:383. Besides cyclohexanone, torsional effects control the stereoselectivity of nucleophilic addition to other cyclic ketones as well, see: Wu YD, Houk KN, Paddon-Row MN. *Angew. Chem., Int. Ed.* 1992; 31:1019.
12. a Anh NT. *Top. Curr. Chem.* 1980; 88:145.b Anh NT, Eisenstein O. *Nouv. J. Chim.* 1977; 1:61.c Anh NT, Eisenstein O. *Tetrahedron Lett.* 1976; 3:155.
13. For reviews, see: Mengel A, Reiser O. *Chem. Rev.* 1999; 99:1191. [PubMed: 11749444]
14. a Bürgi HB, Dunitz JD, Shefter E. *J. Am. Chem. Soc.* 1973; 95:5065.b Bürgi HB, Dunitz JD, Lehn JM, Wipff G. *Tetrahedron*. 1974; 30:1561.c Bürgi HB, Dunitz JD. *Acc. Chem. Res.* 1983; 16:153.
15. Cram DJ, Abd Elhafez FA. *J. Am. Chem. Soc.* 1952; 74:5828.

16. a Karabotsos GJ. *Tetrahedron Lett.* 1972; 52:5289. b Karabotsos GJ, Althuis TH. *Tetrahedron Lett.* 1967; 49:4911. c Karabotsos GJ. *J. Am. Chem. Soc.* 1967; 89:1367.
17. Toromanoff E. *Tetrahedron.* 1980; 36:2809.
18. Fürst A, Plattner PA. *Helv. Chim. Acta.* 1949; 32:275. [PubMed: 18115957]
19. Paddon-Row MN, Rondan NG, Houk KN. *J. Am. Chem. Soc.* 1982; 104:7162.
20. Dannenberg JJ. *Chem Rev.* 1999; 99:1225. [PubMed: 11749445]
21. Electrophiles and cycloaddends: Freeman F. *Chem. Rev.* 1975; 75:439. Allen AD, Tidwell TT. *J. Am. Chem. Soc.* 1982; 104:3145.
22. Nucleophiles: Corey EJ, Shibasaki M, Nicolau KC, Malmstein CL, Samuelson B. *Tetrahedron Lett.* 1976; 17:737. Baldwin SW, Tomesch JC. *J. Org. Chem.* 1974; 39:2382.
23. Radicals: Davies DI, Parrot MJ. *Tetrahedron Lett.* 1972; 13:2719. references therein.
24. a Huisgen R, Ooms PHJ, Mingin M, Allinger NL. *J. Am. Chem. Soc.* 1980; 102:3951. b Huisgen R. *Pure Appl. Chem.* 1981; 53:171.
25. Schleyer P. *J. Am. Chem. Soc.* 1967; 89:701.
26. Schleyer P. *J. Am. Chem. Soc.* 1964; 86:1854.
27. Rondan NG, Paddon-Row MN, Caramella P, Mareda J, Mueller PH, Houk KN. *J. Am. Chem. Soc.* 1982; 104:4974.
28. Houk KN, Rondan NG, G N, Brown FK, Jorgensen WL, Madura JD, Spellmeyer DC. *J. Am. Chem. Soc.* 1983; 105:5980.
29. Huisgen R, Moebius L, Mueller G, Stangl H, Szeimies G, Vernon JM. *Chem. Ber.* 1965; 98:3992.
30. a Gutmiedl K, Wirges CT, Ehmke V, Carell T. *Org. Lett.* 2009; 11:2405. [PubMed: 19405510] b Hansell CF, Espeel P, Stamenovic MM, Barker IA, Dove AP, Du Prez FE, O'Reilly RK. *J. Am. Chem. Soc.* 2011; 133:13828. [PubMed: 21819063] c Watson WH, Galloy J, Bartlett PD, Roof AAM. *J. Am. Chem. Soc.* 1981; 103:2022.
31. Lopez SA, Houk KN. *J. Org. Chem.* 2013; 78:1778. [PubMed: 22764840]
32. a Ess DH, Houk KN. *J. Am. Chem. Soc.* 2008; 130:10187. [PubMed: 18613669] b Ess DH, Houk KN. *J. Am. Chem. Soc.* 2007; 129:10646. [PubMed: 17685614] c Ess DH, Jones GO, Houk KN. *Org. Lett.* 2008; 10:1633. [PubMed: 18363405] d García JI, Martínez-Merino V, Mayoral JA, Salvatella L. *J. Am. Chem. Soc.* 1998; 120:2415. e Sbai A, Branchadell V, Ortuño RM, Oliva A. *J. Org. Chem.* 1997; 62:3049. [PubMed: 11671684]
33. Kobuke Y, Sugimoto T, Furukawa J. *J. Org. Chem.* 1976; 41:1457.
34. Brown FK, Houk KN. *J. Am. Chem. Soc.* 1985; 107:1971.
35. a Lin S, Dudley GB, Tan DS, Danishefsky SJ. *Angew. Chem., Int. Ed.* 2002; 41:2188. b Mandal M, Danishefsky SJ. *Tetrahedron Lett.* 2004; 45:3831. c Mandal M, Yun H, Dudley GB, Lin S, Tan DS, Danishefsky SJ. *J. Org. Chem.* 2005; 70:10619. [PubMed: 16355979]
36. Kohler P, Overman LE, Houk KN. *J. Am. Chem. Soc.* 2012; 134:16054. [PubMed: 22954350]
37. Volp KA, Harned AM. *J. Org. Chem.* Just Accepted.
38. a Meyers AI, Seefeld MA, Lefker BA. *J. Org. Chem.* 1996; 61:5712. b Thottathil JK, Moniot JL, Mueller RH, Wong MKY, Kissick TP. *J. Org. Chem.* 1986; 51:3140.
39. a Meyers AI, Seefeld MA, Lefker BA, Blake JF. *J. Am. Chem. Soc.* 1997; 119:4565. b Meyers AI, Seefeld MA, Lefker BA, Blake JF, Williard PG. *J. Am. Chem. Soc.* 1998; 120:7429.
40. Ando K, Green NS, Li Y, Houk KN. *J. Am. Chem. Soc.* 1999; 121:5334.
41. Leanna MR, Martinelli MJ, Varie DL, Kreea TJ. *Tetrahedron Lett.* 1989; 30:3935.
42. Martinelli MJ, Peterson BC, Khau VV, Hutchison DR, Leanna MR, Audia JE, Droste JJ, Wu Y-D, Houk KN. *J. Org. Chem.* 1994; 59:2204.
43. Lucero MJ, Houk KN. *J. Org. Chem.* 1998; 63:6973. [PubMed: 11672319]

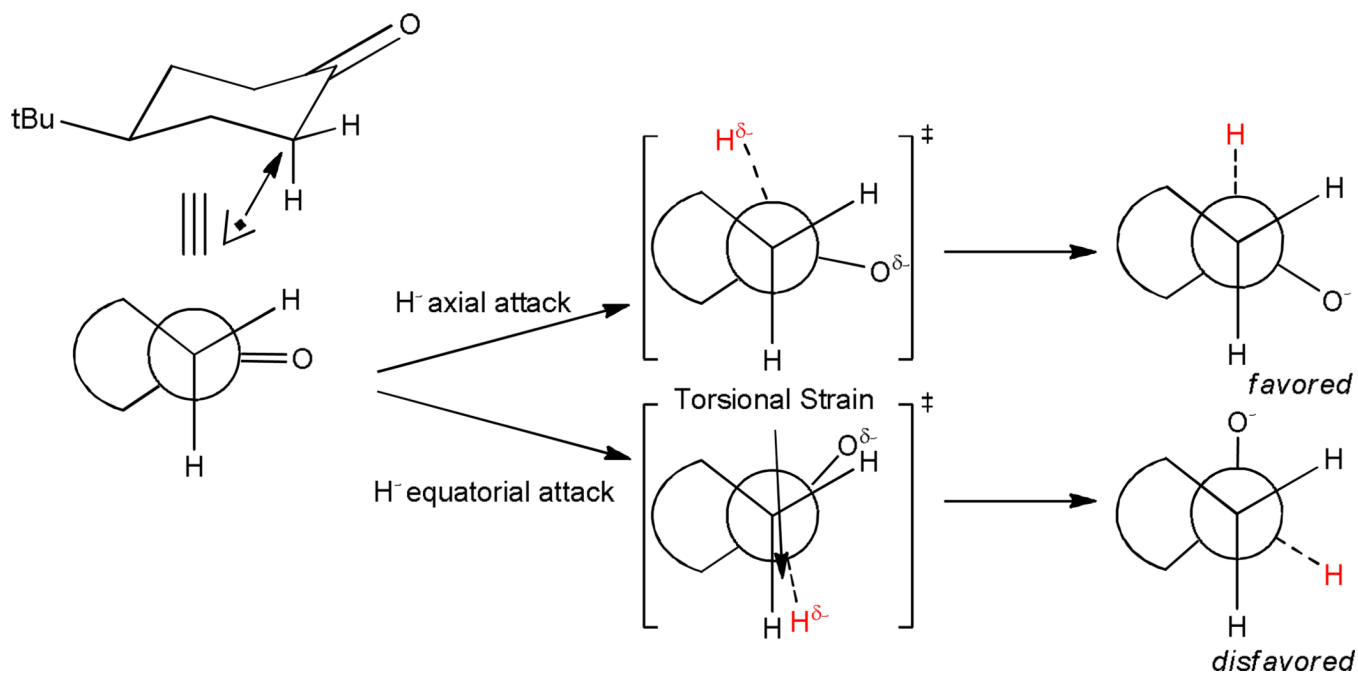


Figure 1.
Reduction of 4-tert-butylcyclohexanone with hydrides.

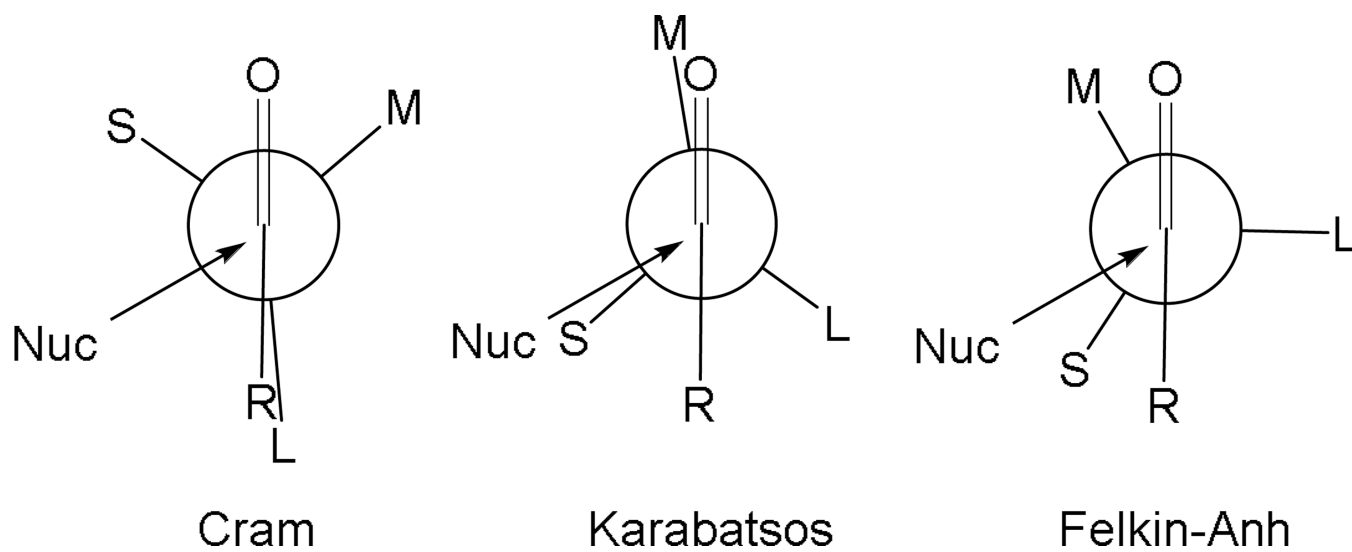


Figure 2. Summary of the models for nucleophilic attack on carbonyl compounds.

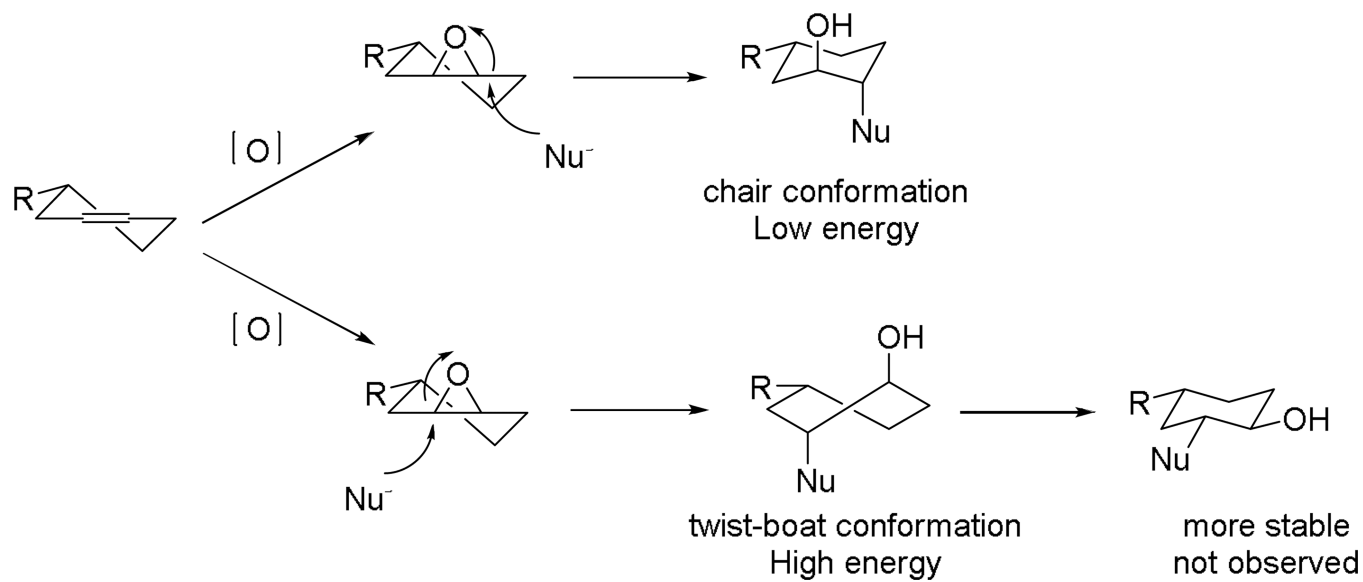


Figure 3.
Furst-Plattner rule.



norbornene

1

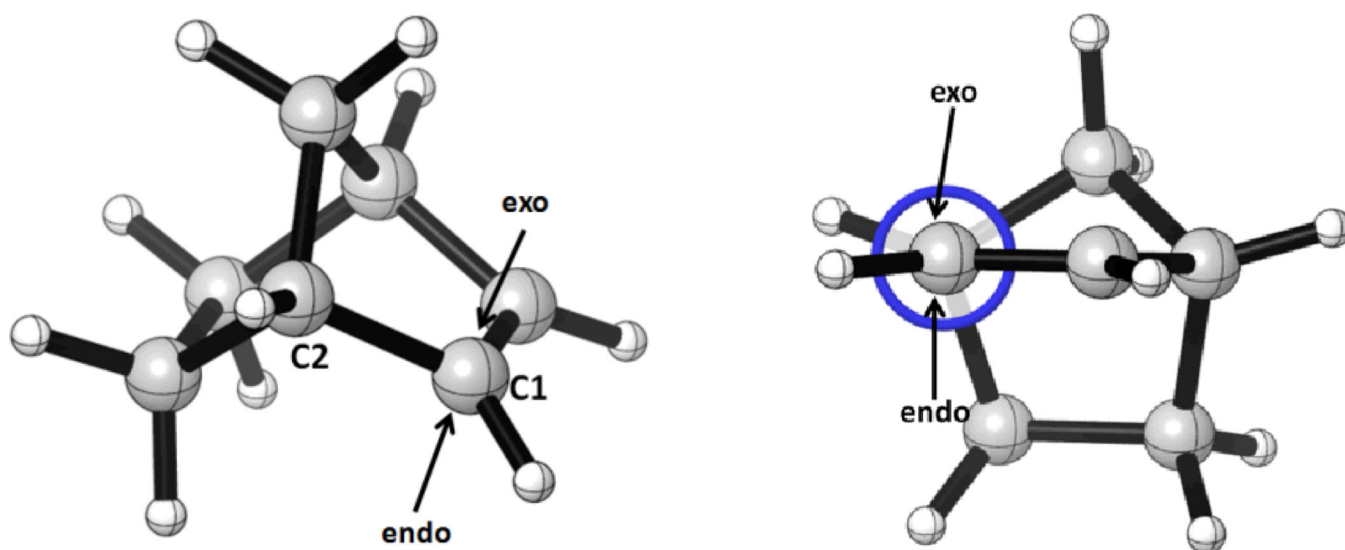


Figure 4.
Optimized structures of norbornene **1** (Left: top view; Right: side view).

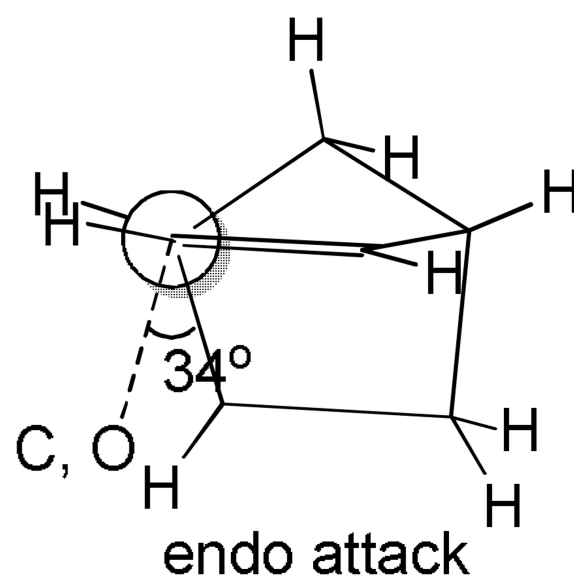
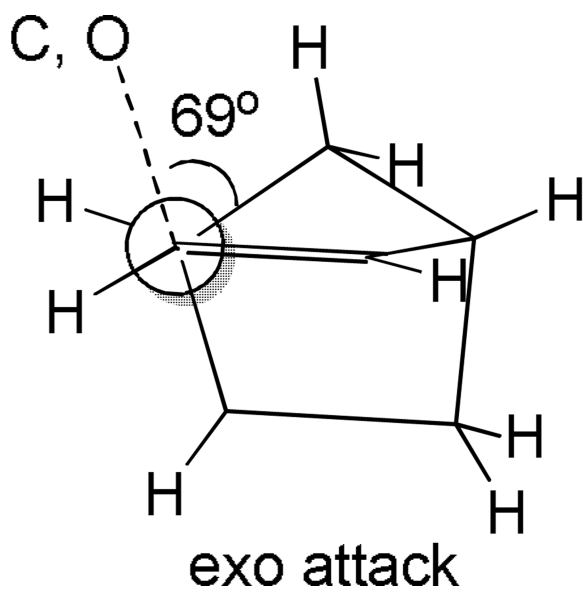


Figure 5.
Transition structures showing direction of bond formation for attack of C or O of fulminic acid on norbornene.

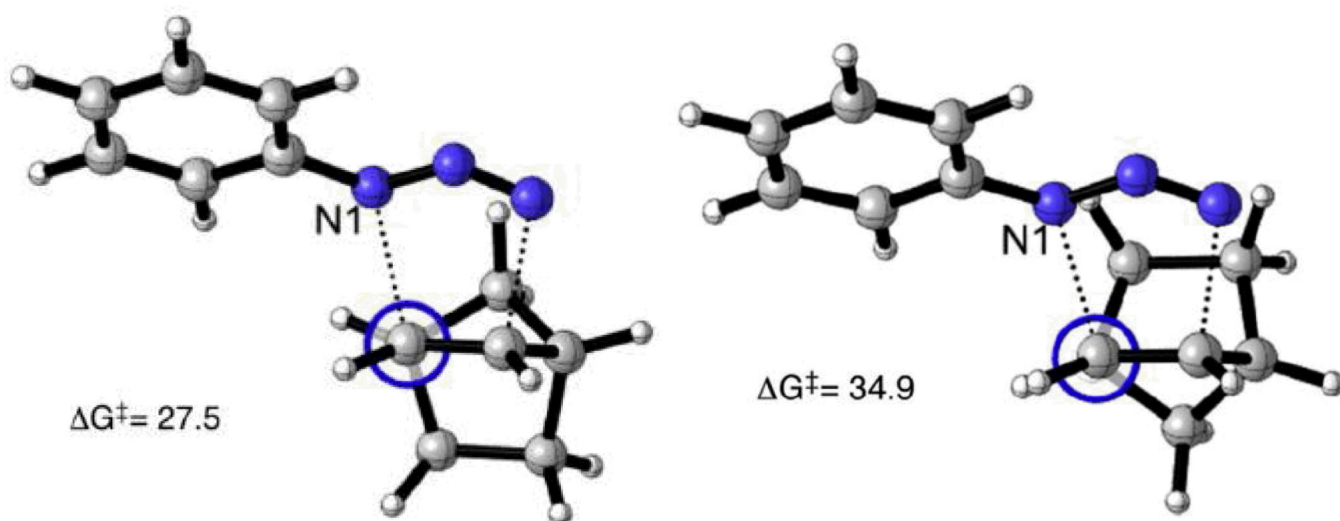


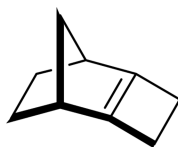
Figure 6. Newman projections for the cycloadditions of phenyl azide to exo (left) and endo (right) faces of norbornene. Image reproduced with permission from ACS Journals and the authors.

**2****TS2-exo**

$$\Delta G^\ddagger = 16.0 \text{ kcal/mol}$$

TS2-endo

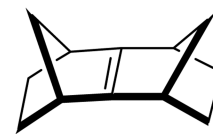
$$\Delta G^\ddagger = 21.6 \text{ kcal/mol}$$

**3****TS3-exo**

$$\Delta G^\ddagger = 22.1 \text{ kcal/mol}$$

TS3-endo

$$\Delta G^\ddagger = 30.8 \text{ kcal/mol}$$

**4****TS4-exo**

$$\Delta G^\ddagger = 26.2 \text{ kcal/mol}$$

TS4-endo

$$\Delta G^\ddagger = 40.3 \text{ kcal/mol}$$

Figure 7. Other norbornene derivatives studied and activation energies for their cycloadditions with phenyl azide.

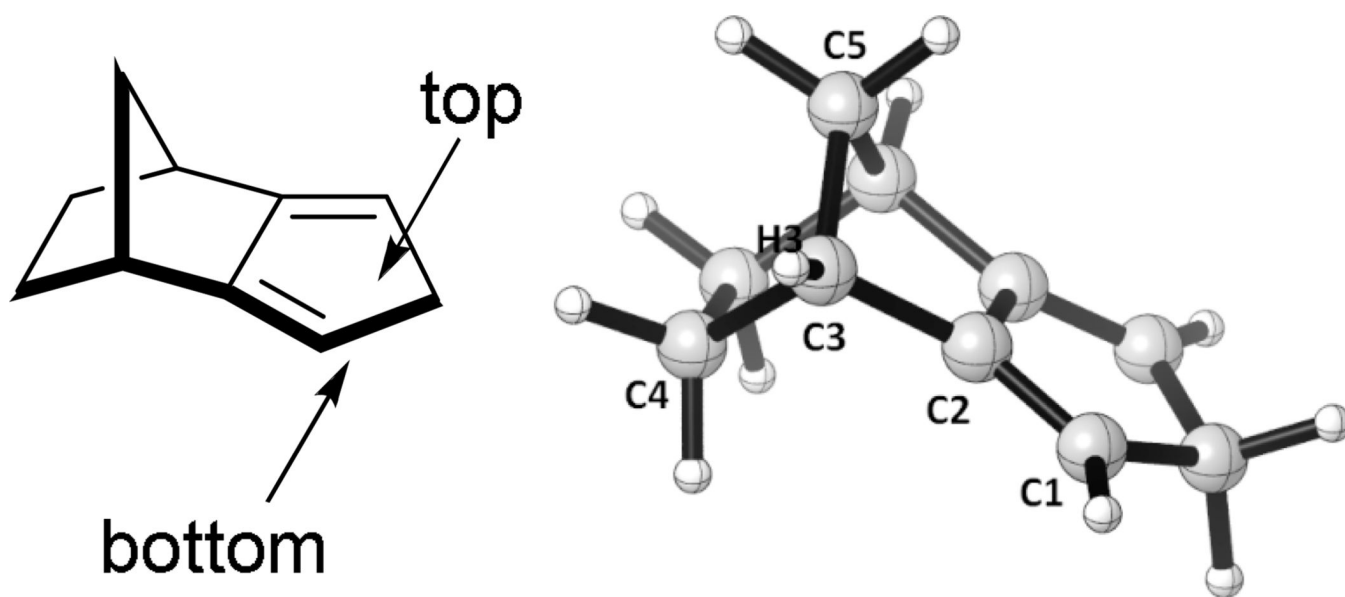


Figure 8.
Optimized structure of isodicyclopentadiene.

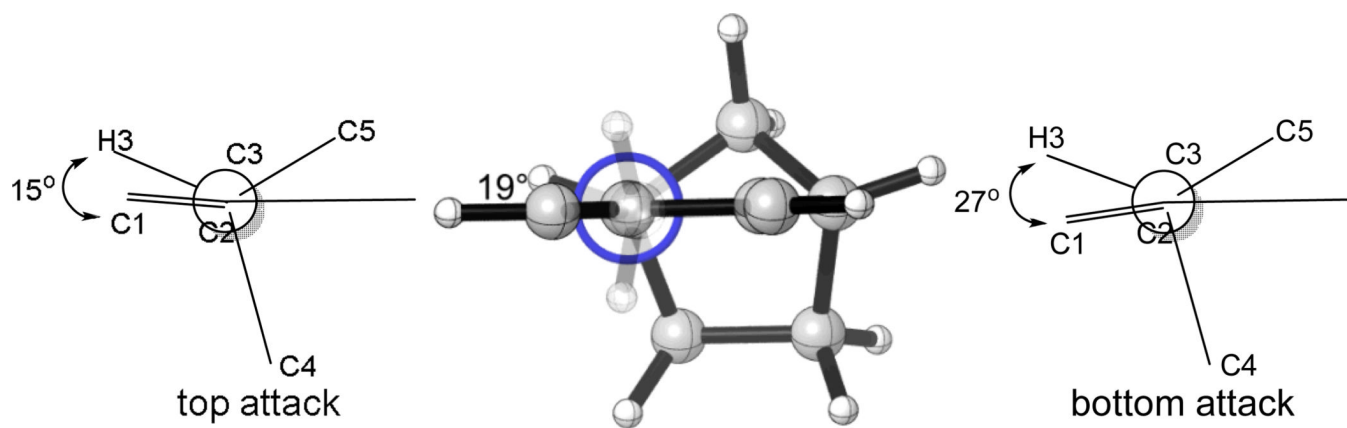


Figure 9.
Newman projections of Diels-Alder reaction of isodicyclopentadiene with ethylene.

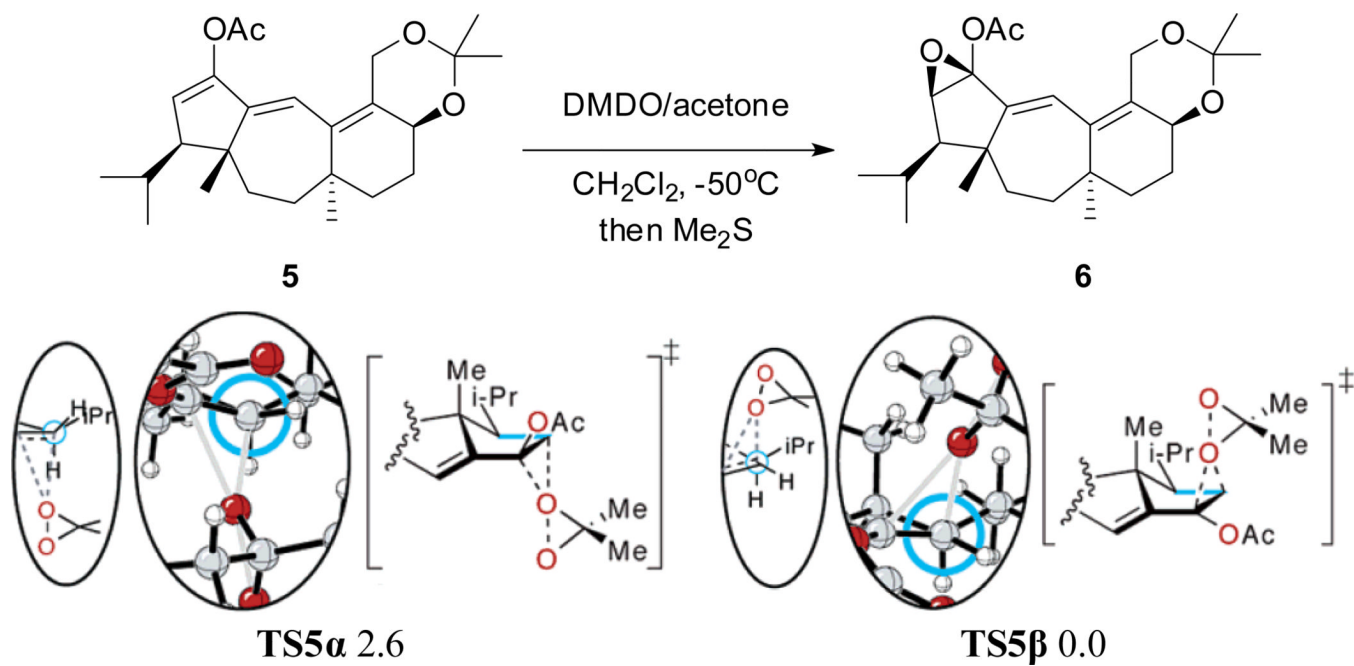


Figure 10. Asymmetric epoxidation of a guanacastepene **A** precursor and transition structures of **TS5 α** and **TS5 β** . Newman projections of the highlighted blue bond are shown in the oval insets. Image reproduced with permission from ACS Journals and the authors.

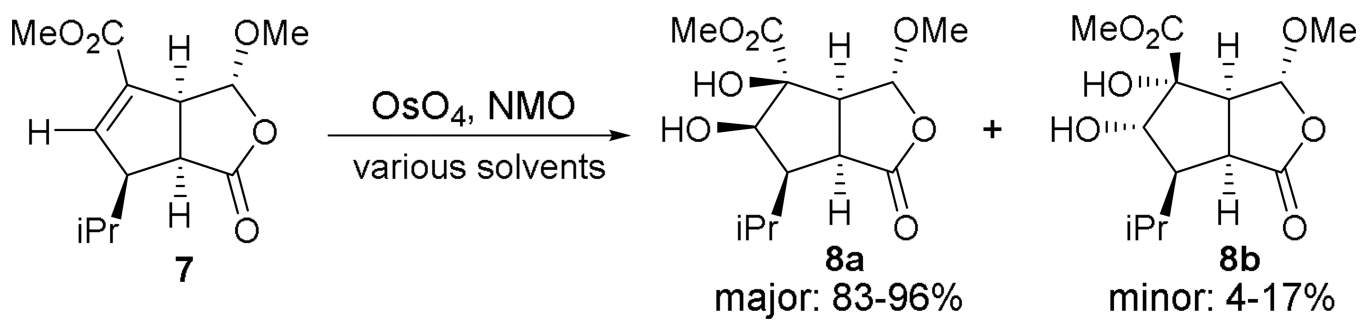


Figure 11. Dihydroxylation of cis-oxabicyclo[3.3.0]octenone **7** with OsO_4 .

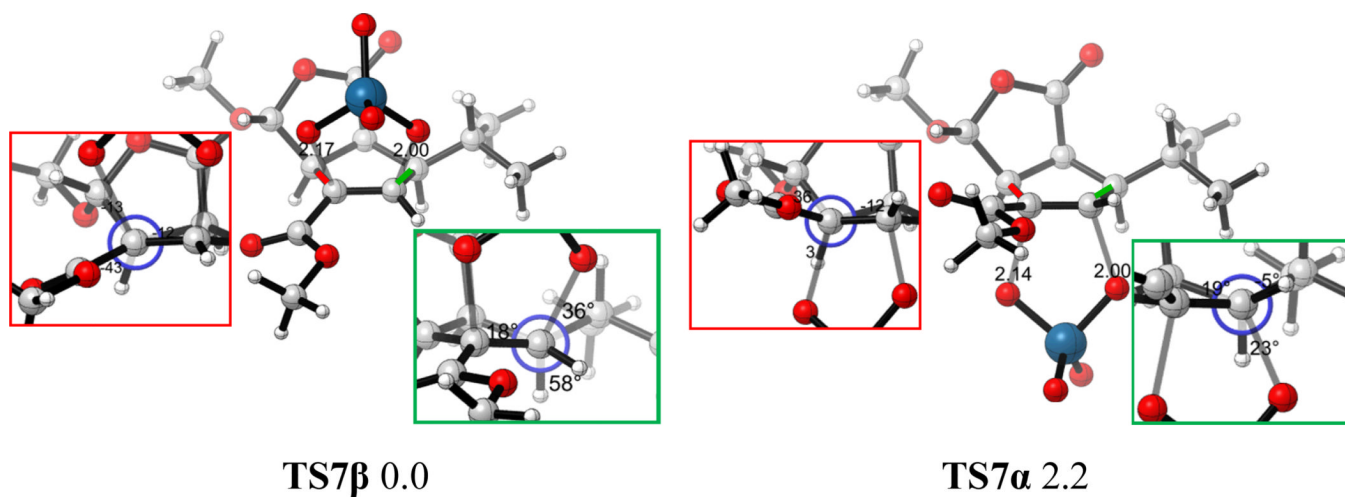


Figure 12. Optimized β and α -dihydroxylation transition structures of *cis*-oxabicyclo[3.3.0]octanone 7. Image reproduced with permission from ACS Journals and the authors.

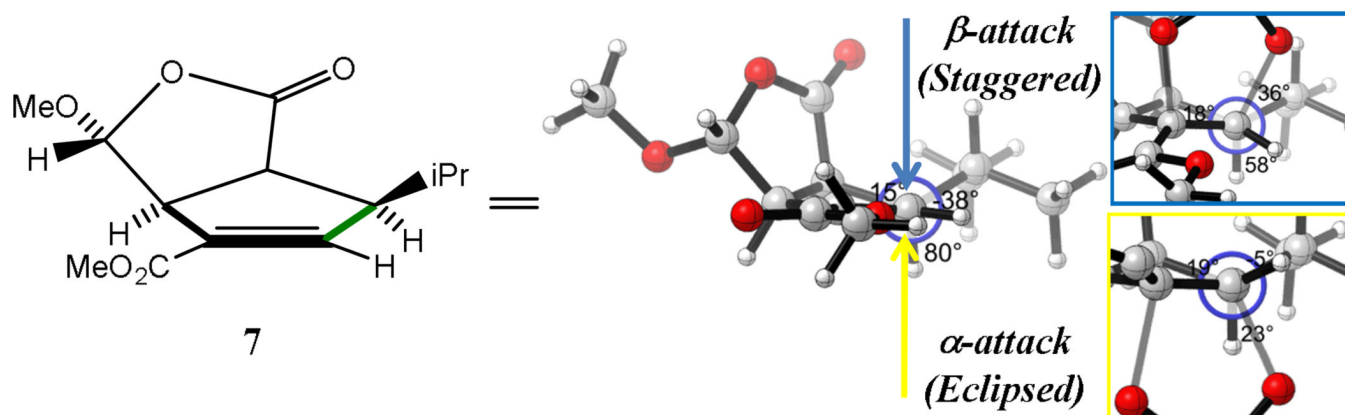


Figure 13. Optimized structure of *cis*-oxabicyclo[3.3.0]octenone **7**. Newman projections shown in the blue and yellow box insets illustrate the resultant torsional effects for the β and α -dihydroxylation transition states. Image reproduced with permission from ACS Journals and the authors.

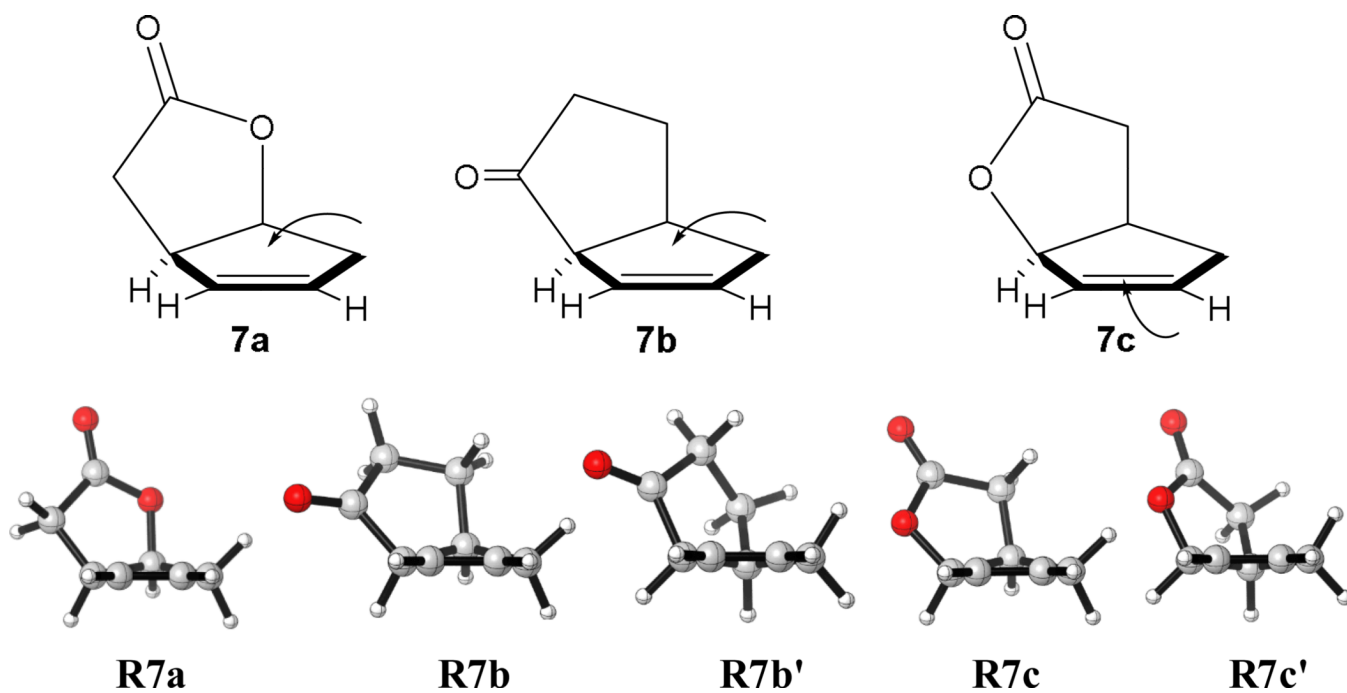


Figure 14.
Three fused cyclopentene compounds and their optimized geometries.

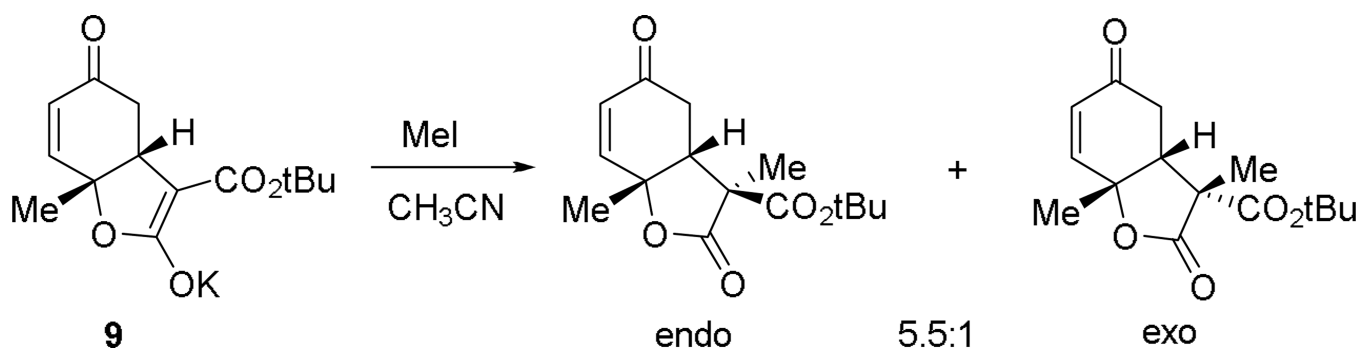


Figure 15.
Alkylation of bicyclic malonates **9** with MeI.

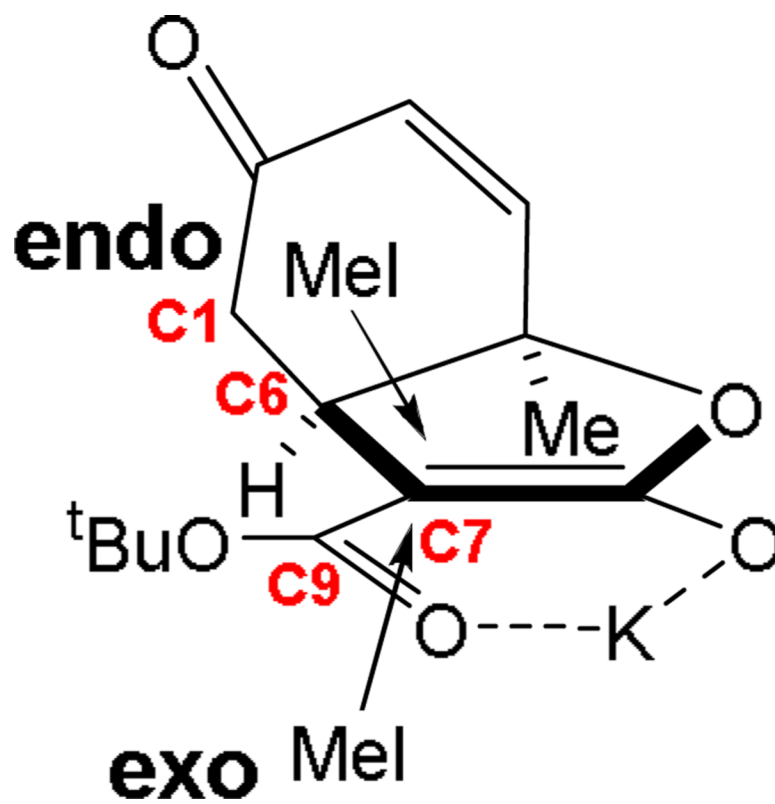


Figure 16.
Endo and exo-alkylation approaches of MeI to bicyclic malonates **9**.

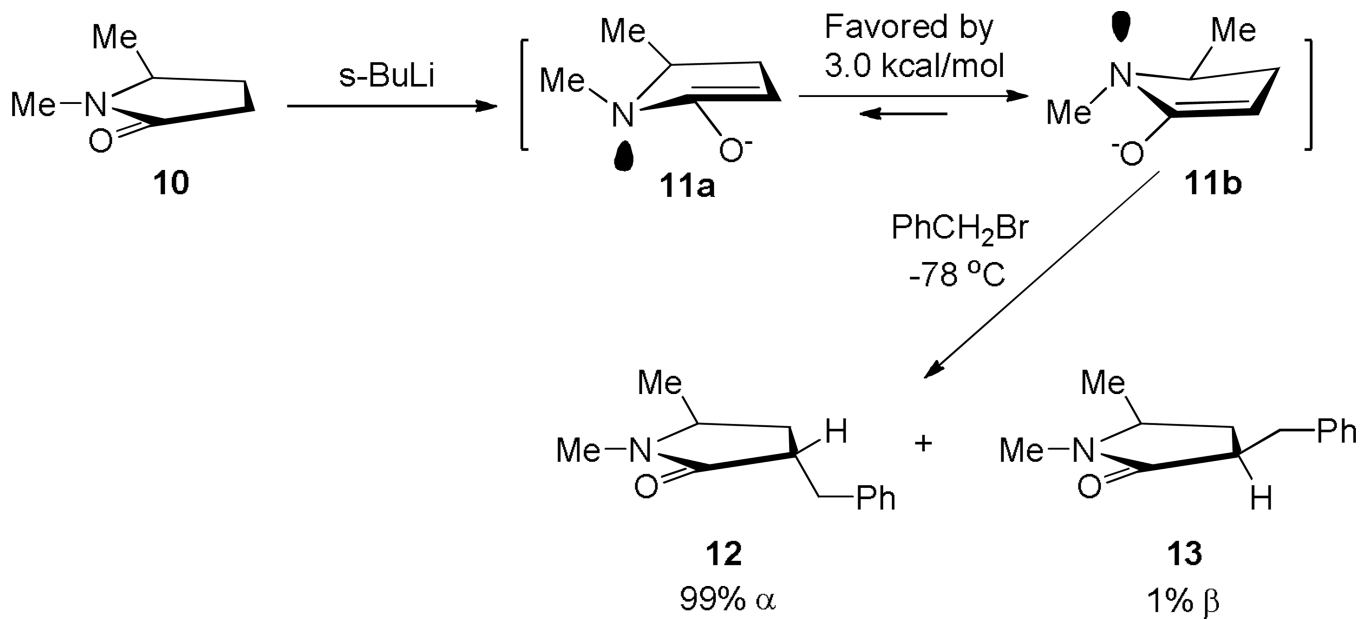


Figure 17.
Alkylation of pyrrolidinone **10** with benzyl bromide.

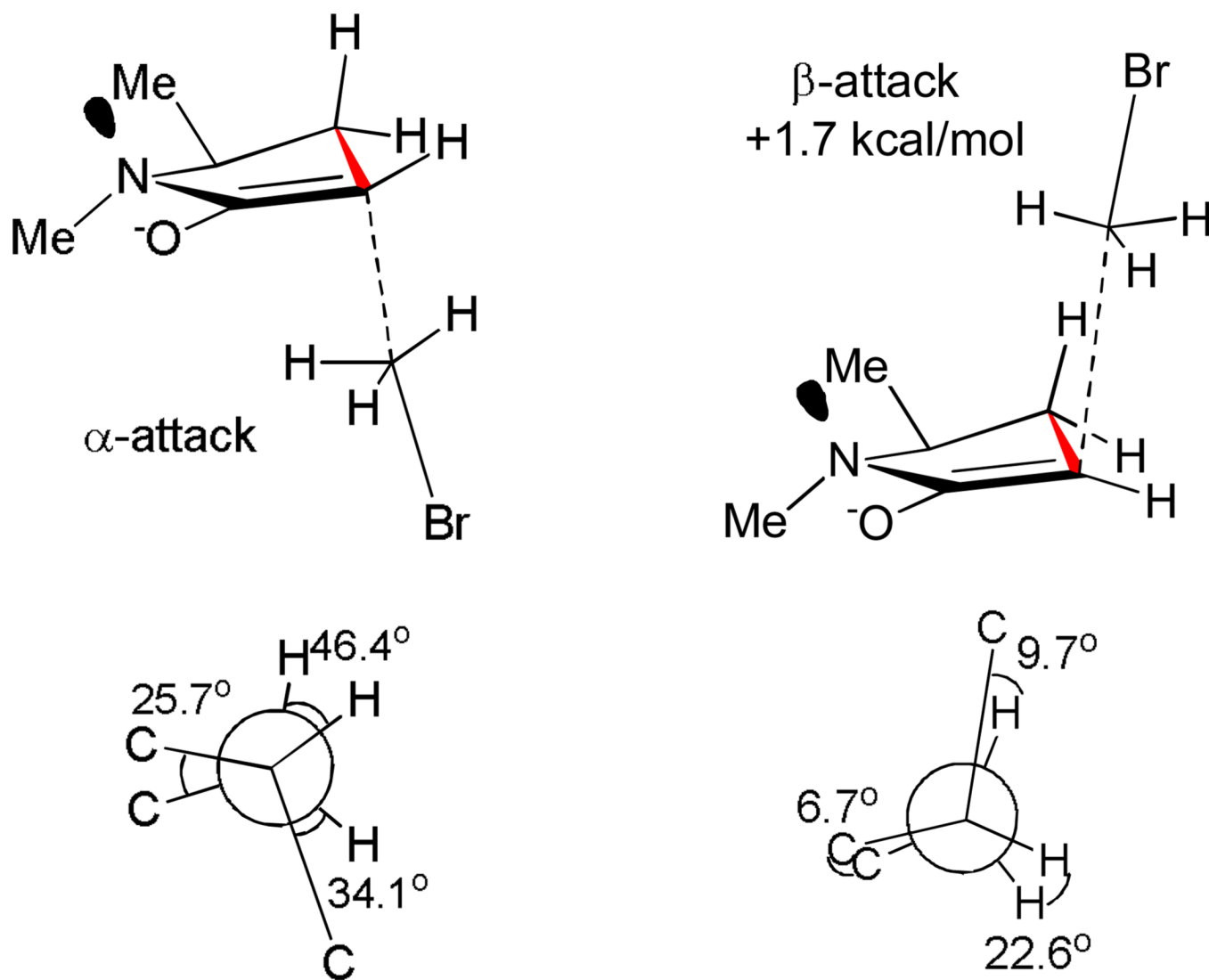
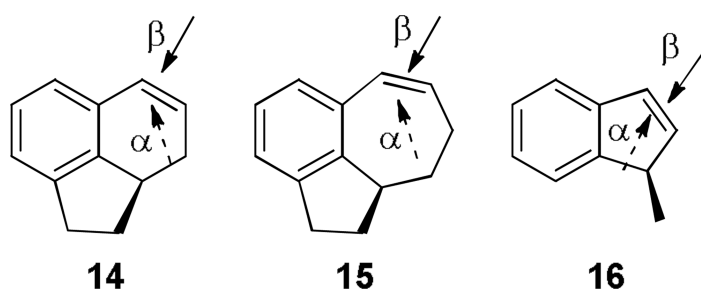


Figure 18.
Optimized transition structures of α - and β -alkylation of pyrrolidinone enolate **11b**.
Newman projections are viewed from the highlighted red bond.



	14	15	16
m-CPBA	1/99	82/18	50/50

Figure 19.
 β/α ratios observed in the epoxidations of styrene derivatives **14**, **15** and **16**.

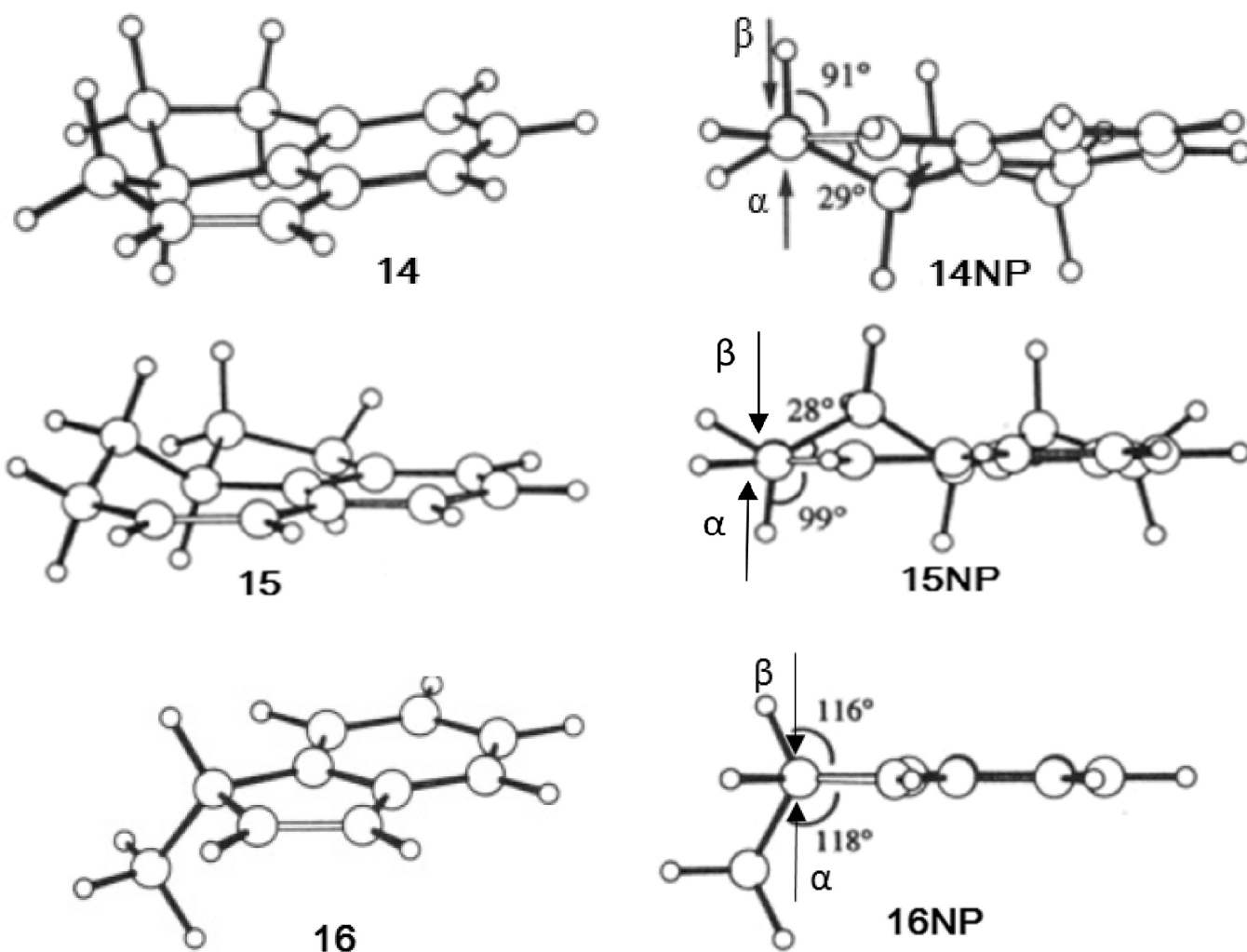


Figure 20. MM2 optimized structures of compounds **14**, **15** and **16**. Structures **14NP**, **15NP** and **16NP** are Newman projections. Figure is reproduced by permission of ACS.

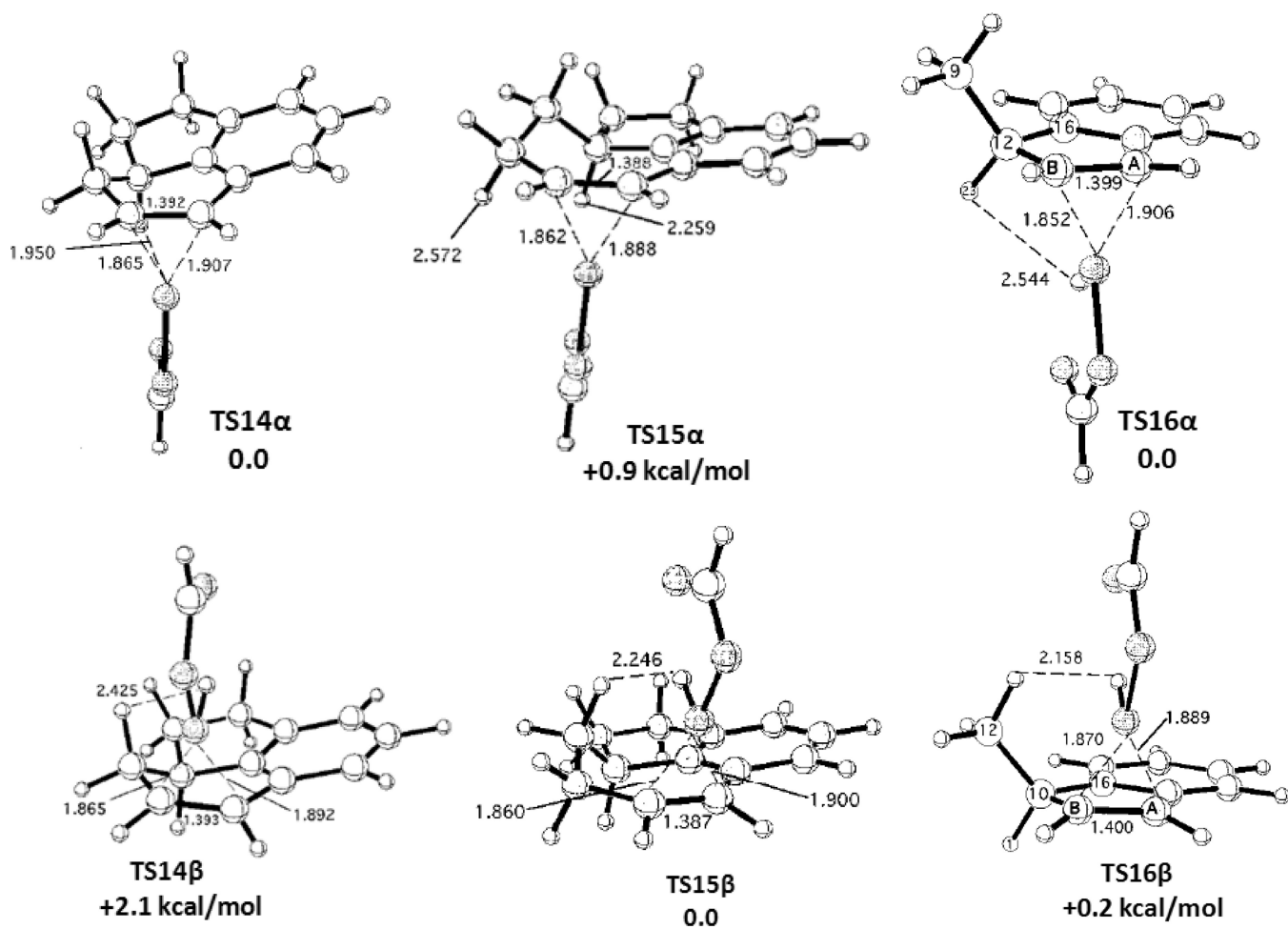


Figure 21. PM3 optimized transition structures of performic acid epoxidation of **14**, **15** and **16**. Single point energy calculations were performed using RHF/6-21G*. Image reproduced with permission from ACS Journals and the authors.